Fouling study in submerged PVDF ultrafiltration for refinery produced wastewater treatment: Effect of suspended solids concentration and aeration

E. Yuliwati[1,2,3], A.F. Ismail[1,2,*], M.A. Kassim[1,2], T. Matsuura[1,4]

[1]Advanced Membrane Technology Research Centre (AMTEC),
[2]Faculty of Petroleum and Renewable Energy Engineering,
Universiti Teknologi Malaysia, 81310 UTM, Skudai Johor, Malaysia
Tel. +60 (7) 553-5592; Fax: +60 (7) 558-1463
[3]Department of Industrial Engineering, Faculty of Engineering
Universitas Bina Darma, 30251 Palembang, Indonesia
Tel. +62 (711) 515-679; Fax: +62 (711) 518-000
[4]Department of Chemical Engineering, Industrial Membrane Research Laboratory, University of Ottawa, Ont., Canada KIN 6N5
*Corresponding author: afauzi@utm.my

Abstract – Fouling behavior for modified polyvinylidene fluoride (PVDF) hollow fibers fouled with suspended solid matter was investigated. This study describes the effect of aeration to prevent the membrane fouling. Hollow fiber membranes were spun by a dry-jet wet phase inversion spinning process. Addition of lithium chloride monohydrate ($LiCl.H_2O$) and titanium dioxide (TiO_2) nanoparticles concentration in the spinning dope improved the hydrophilicity, average pore size, porosity, surface roughness, and resulted in increasing the fouling resistance of membrane, which confirmed by water permeation. Distinctive changes were observed in membrane characteristics in terms of ionizable functional groups, membrane structural, wettability, and roughness measurement. Fouling characteristics of synthetic refinery wastewater with mixed liquor suspended solids (MLSS) concentration of 3 g/L and 4.5 g/L were assessed by filtering the feed water using submerged PVDF membrane with varied aeration flow rate (ABFR) (1.2, 2.4, and 3.0 mL/min). Response surface methodology (RSM) was used to determine the optimal operating conditions for refinery produced wastewater treatment. Results showed that the flux and total suspended solids (TSS) removal were 148.82 L/m^{2}h and 99.82%, respectively. Meanwhile, optimum operating conditions were MLSS of 3.0 g/L, ABFR of 2.4 mL/min, and hydraulic retention time (HRT) of 276.93 min.

Keywords: Submerged ultrafiltration; Fouling; Suspended solids; Aeration.

1. Introduction

Low pressure membrane processes such as ultrafiltration (UF) is being increasingly used for wastewater treatment. The properties of feed have also a major impact on membrane fouling. However, fouling, which can affect the permeate quality and operating cost, is a major limitation for their broader implementation. Particulate matter, inorganic and organic materials are potential contributors to membrane fouling in refinery wastewater treatment [1-3]. A fouling layer, composed of suspended solids, inorganic and organic complexes forms on the membrane surface. The properties of this fouling layer largely control the membrane performance. Preventing or reducing of the formation of this fouling layer by using aerated filtration system, could enhance the performance of the membrane processes. The

reversibility of fouling to be dependent on hydrodynamic conditions and physicochemical properties [4-7].

The effect of continuously aeration on fouling layer in submerged membrane ultrafiltration has been also discussed by several researchers [8-11]. However, the informations of these effects have been identified unclearly.

The aim of this study was to investigate the effect of suspended solids (mixed liquor suspended solids (MLSS)) concentration and aeration (air bubble flow rate (ABFR)) on flux and fouling reversibility. The more understanding of the fouling mechanism and optimized process conditions for refinery wastewater treatment using submerged ultrafiltration was described clearly.

2. Experimental

2.1. Materials

Ultrafiltration membranes have been prepared using Kynar®740 PVDF polymer pellets which were purchased from Arkema Inc., Philadelphia, USA. The solvent N,N-dimethylacetamide (DMAc,Aldrich Chemical) (Synthesis Grade, Merck, 99%) was used as polymer solvent without further purification. Lithium chloride monohydrate ($LiCl{\cdot}H_2O$) and nanoparticles titanium dioxide (TiO_2) were used as inorganic additives. Both chemical additives were purchased from Sigma-Aldrich and used as received. Glycerol was purchased from MERCK (Germany) and used as non-solvent for the post treatment of membrane. In all cases, tap water was used as the external coagulation bath medium in the spinning process.

2.2. Membrane preparation

An amount of pre-dried (24 h oven dried at 50 °C) PVDF pellets was weighed and poured into pre-weighed DMAc solvent. The mixture was stirred to ensure thorough wetting of polymer pellets, prior to the addition of appropriate amount of LiCl·H2O at 50 °C. TiO_2 was added to the polymer dope mixtures which were continuously stirred for 48 h (IKA-20-W) at 500 rpm until a homogenous solution was formed. The polymer solution was kept in a glass bottle and air bubbles formed in the dope were removed using water aspirator for several hours. The fully dissolved polymer solution was transferred to a stainless steel reservoir, allowed to stand and degassed for 24 h at room temperature prior to the spinning process.

PVDF hollow fiber UF membranes were spun at room temperature by a dry-jet wet spinning method. The spinning solutions were divided into two batches. Membranes were prepared from 19 wt.% PVDF in DMAc at different TiO_2 concentrations (0, 10, 20 wt.%) and $LiCl{\cdot}H_2O$ was maintained at 5.2 wt.% of the weight of the PVDF, as shown in previous study respectively [12]. In general, the polymer solution was pressurized through spinneret with controlled extrusion rate, while the internal coagulant was adjusted at 1.4 mL/min. The hollow fiber that emerged from the tip of the spinneret was guided through the two water baths at a take up velocity of 13.7 cm/s, carefully adjusted to match the free falling velocity before it landed in a final collection bath to complete the solidification process. The spun hollow fibers were immersed in the water bath for a period of 3 days, with daily change of the water, to remove the residual DMAc and the additives. The hollow fibers were then post-treated using 10 wt.% glycerol aqueous solution as a non-solvent exchange for 1 day in order to minimize fiber shrinkage and pore collapse. After the fibers were dried for 3 days, they were ready for making hollow fiber test modules.

2.3. Submerged ultrafiltration process

The permeation flux and rejection of PVDF hollow fiber membranes for synthetic refinery wastewater, as listed in Table 1, were measured by submerged ultrafiltration experimental equipment as shown in Fig. 1 [13].

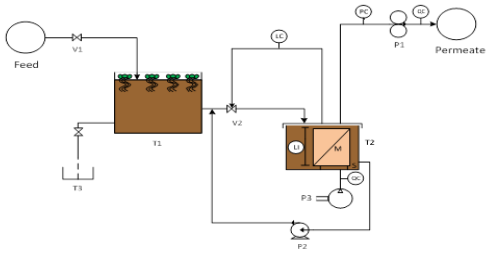

Fig.1: Submerged ultrafiltration system for refinery wastewater treatment (V_1: wastewater valve, T_1: pretreatment tank, V_2:feed membrane reservoir valve, S: sparger, M: membrane module, T_2: feed reservoir, T_3: effluent tank, P_1: peristaltic pump, P_2: centrifugal pump, P_3: air pump, QC: flow control, LC: liquid control, LI: level indicator, PC: pressure control.

Two in-house produced U-shape hollow fiber modules, with a filtration area of 22.46 dm^2, were submerged in prepared suspension in membrane reservoir with volume of 14 L. A cross-flow stream of aeration was produced by air bubbling generated by a diffuser situated underneath the submerged membrane module. The air bubble flow rate per unit projection membrane area was set at 1.2, 2.4, and 3.0 mL/min in order to maintain proper turbulence. The filtration experiments were carried out in vacuum condition created using a peristaltic pump (Master flex model 7553-79, Cole Palmer) with permeate that being withdrawn from the open end of fibers.

Table 1: Composition of synthetic refinery wastewater with standard deviation (S.D.) and Standard B of national standard for wastewater and water discharged [14].

Constituent, unit	Concentration (S.D.)	Standard B
pH	6.7	5.5 – 9.0
COD, mg/L	555.0 (0.25)	200
NH_3-N, mg/L	29.1 (1.02)	20.0
Suspended Solid, mg/L	213.0 (0.07)	100.0

Source: Parameter Limits of Effluent of Standard B Environmental Quality Regulation 2009.

The liquid level in the feed tank was maintained constant throughout experiment. The air scouring bubble generated was advantageous to exert shear stress to minimize particles deposited on the membrane surface during filtration process. The volume of the water permeation collected was determined using a graduated cylinder. After completing filtration, the membrane surface was cleaned with alkaline solution to remove the particle-packed layer which might form during filtration.

2.4. Membrane characterizations

The morphologies of outer surfaces and cross sections of membranes were examined by a field emission scanning electron microscope (FESEM) (JEOL JSM-6700F), which were taken at various magnifications. Samples were prepared by fracturing the membranes in liquid nitrogen. All specimens were freeze-dried and coated with a thin layer of gold using a sputter coater before observation. The AFM images were obtained over different areas of each hollow fiber membrane using a tapping mode Nanoscope III equipped with 1553D scanner (SPA-300 HV,USA). In this study, scans were made on areas of 5 μm × 5 μm. The AFM analysis software program allowed computation of various statistic related to the surface roughness on predetermined scanned membrane area [15].

Asymmetric porous membranes were characterized by determination of porosity and average pore radius. The membrane porosity, ε, was defined as the volume of the pores divided by the total volume of the porous membrane. The membrane porosity was calculated using the following equation,

$$\varepsilon = \frac{\dfrac{(w_1 - w_2)}{\rho_W}}{\dfrac{(w_1 - w_2)}{\rho_W} + \dfrac{w_2}{\rho_P}} \text{ x } 100 \qquad (3)$$

where ε is the porosity of the membrane (%), w_1 the weight of wet membrane (g), w_2 the weight of dry membrane (g), ρ_p the density of the polymer (g/cm^3) and ρ_w is the density of water (g/cm^3).

Average pore radius, r_m, was investigated by filtration velocity method. According to Guerout-Elford-Ferry Equation, r_m could be calculated:

$$r_m = \sqrt{\frac{(2.9 - 1.75\varepsilon) x 8\eta \ell Q}{\varepsilon x A x \Delta P}} \qquad (4)$$

where η is water viscosity (8.9 x 10^{-4} Pa s), ℓ is the membrane thickness (m), ΔP is the operation pressure (0.1MPa), ε is the porosity of the membrane (%), Q is volume of permeate water per unit time (m^3 s^{-1}), A is an effective area of membrane (m^2).

The breaking strain and strength of the membranes were examined to investigate the mechanical stability using a tensile tester (LRX2 SKN LLYOD) instrument at room temperature. Tests were conducted on a cross head speed of 20 mm min^{-1} at break and gate length of filament at 25 mm [16]. At least five measurements were performed for each membrane sample and the average values are reported in this study.

Table 2 shows the PVDF membranes and operating characteristics of the submerged ultrafiltration [17]. In order to enhance membrane hydrophilicity, $LiCl.H_2O$ was added during membrane preparation process with the effort to improve membrane water productivity.

Table 2. Membrane properties and operating characteristics of the submerged ultrafiltration.

Parameter	**Membrane**
Membrane configuration	Hollow fiber
Membrane material	PVDF
Hydrophilic additive added	LiCl and TiO_2
Outer diameter (mm)	1.1
Inner diameter (mm)	0.55
Pore size (nm)	34.05
Tensile strength (MPa)	3.37 ± 0.13
pH feed solution (pH)	6.7
ABFR (mL/min)	1.2, 2.4, 3.0
MLSS concentration (g/L)	3.0 and 4.5

2.5. Effect of suspended solids concentration on membrane performance

Effect of MLSS concentration on submerged membrane UF fouling is not as obvious as ABFR effects, mainly due to the complexity and variability of the biomass components. While the extrapolymer substances and other biomass

characteristics are not accounted, the increase in MLSS concentration alone has a mostly negative effect on the flux obtained in a SS-MBR [18], the stabilised permeation rate [19], and on the limiting flux [20]. Although the same type of membrane was used in both studies and the hydraulic condition were similar, flux values reported by Sablani *et al*. (2001) and Oh *et al*. (2009) differ significantly, namely, 621 L/m^{2}h for MLSS of 4 g/L and 221 L/m^{2}h for MLSS of 2.5 g/L respectively [21,22]. This observation demonstrates the importance of carrying out tests under the same conditions for assessing hydraulic/hydrodynamic parameter and impacts.

2.6. Effect of aeration on membrane performance

An increase in ABFR and thus cross flow velocity (CFV) supresses fouling and increases the flux. Although most of the studies on flux are based on sidestream (SS) operation, studies carried out with submerged membrane UF or with ideal feed solutions suggest that an increase in air flow rate at the membrane surface limits fouling [23]. However, Profio *et al.,* (2011) observed an optimum aeration rate beyond which a further increase has no effect on fouling suppression. Details of the phenomena occuring during air sparging have been extensively reported [24].

2.7. Response Surface Methodology (RSM)

RSM is a collection of mathematical and statistical techniques, commonly used for improving and optimizing processes. It can be used to evaluate the relative significance of several affecting factors in the presence of complex interactions. This methodology optimizes the flux and TSS removal in submerged hollow fiber membrane process. Design expert 8.0.5.2 software (trial version) is used for the statistical design of experiments and data analysis and performed in duplicate [25]. In this study, the quartic model used for predicting the optimal point was according as follows

$$y(x) = \sum_{i=1}^{N} e_i x_i^4 + + \sum_{ij(i<j)}^{N} e_{ij} x_i^3 x_j + \sum_{ij(i<j)}^{N} e_i x_i^2 x_j^2 + \sum_{ijk(i<j<k)}^{N} e_{ijk} x_i^2 x_j x_k + \sum_{ijkl(i<j<k<l)}^{N} e_{ijkl} x_i x_j x_k x_l \quad (4)$$

where y is the response variable, e_i, e_{ij}, e_{ijk}, and e_{ijkl} are the polynomial coefficients of the model, $x_i x_j x_k$ and x_l are the coded levels of the independent variables [30].

3. Results and Discussion

3.1. Microscopic analysis using FESEM and AFM

Figs. 2 and 3 show the FESEM micrographs of the clean and fouled PVDF hollow fibers. FESEM images of fouled membranes are shown in Fig. 3. In this figure, majority of large pores are not visible anymore due to the presence of particles of different shapes and sizes combined with an polymer matrix. The layer is relative porous contrary to that observed for Fig. 3b, in which a thicker and denser surface layer, which consists of many particles of suspended solids and aggregates are observed. This is caused by a progressive penetration in the pores of small particles of equivalent size (cell fragments) and some dissolved macromolecules.

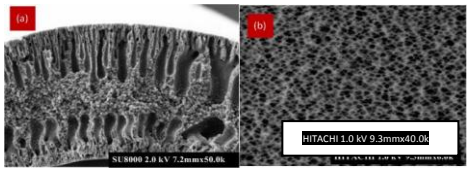

Fig.2. FESEM images of the (a) cross-section (Mag. 500x) and (b) outer surface (Mag. 40.0kx) of cleaned PVDF membranes.

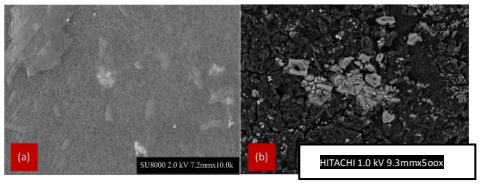

Fig. 3. FESEM images of the outer surface of fouled PVDF membranes (Mag. 500x) at the refinery produced wastewater with MLSS concentration of (a) 3 g/L (b) 4.5 g/L.

Additionally, the membranes surface topographies of 3-D images were also observed using AFM. The high peaks seen as bright regions in the AFM images characterize the nodules while the pores are seen as dark depressions. As shown in Fig. 4, the AFM images revealed that the outer surfaces of clean membranes have nodule-like structures. After filtration, the outer surface of both membranes seemed smoother which were promoted by filtration cake. The feed solution with *MLSS* concentration of 4.5 g/L has larger grains than those of 3 g/L due to the deposited foulants on the surface. The size of nodule aggregates increased on both of fouled surfaces as shown in Figs. b-1,-2. These results indicate that more *MLSS* concentration in the feed solution promoted the more significant irreversible fouling, faster reversible cake establishment and consequently decreased the permeate flux during filtration. This agrees with the study by Mo *et al.*, (2008) that showed suspended solids participated in the membrane fouling, which caused the deposition, pore blocking and irreversible fouling [26]. This could promote the formation of a filtration cake at the beginning of filtration due to the reduction of

pore density and pore diameter of the outer surface membrane.

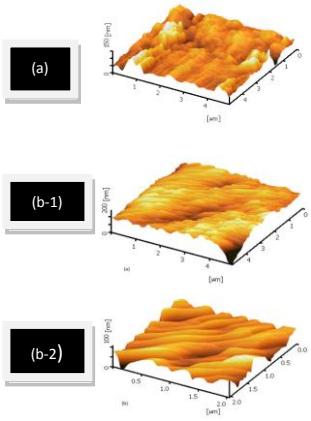

Fig. 4. 3D-AFM images of the outer surface (a) clean membrane, (b-1) fouled membranes with MLSS concentration of 3 and (b-2) 4.5 g/L.

3.2. Statistical analysis using RSM

In the present work, the relationship between three factors (ABFR, HRT, and MLSS concentration) and two responses (flux and TSS removal efficiency) for submerged hollow fiber membrane is analyzed using RSM. Significant model terms are desired to obtain a good fit in a particular model. In this study, the backward elimination procedure was employed to eradicate the insignificant terms and ANOVA results of this backward quartic model.

3.2.1. Effect of MLSS concentration on membrane performance

The enhancement brought by increasing TSS removal appears to be greater at higher HRT of 300 min. The effects of MLSS and HRT on TSS removal depicted in Figs. 5 demonstrated that the TSS removal decreased when MLSS changed from 3.00 to 6.00 g/L. It is worth to note that increase in HRT at low level MLSS concentration (3.00 g/L), resulted in increase of TSS removal, however lower suspended solid removal was applied at high level MLSS concentration (6.00 g/L), suggesting that the performance of process applied was essentially influenced by MLSS concentration variable. A highest peak at approximately HRT of 273 min and MLSS of 3.00 g/L was observed in the resulted TSS removal 3D-plot. It can be concluded that an increase in TSS removal occurred with increasing HRT and decreasing MLSS concentration.

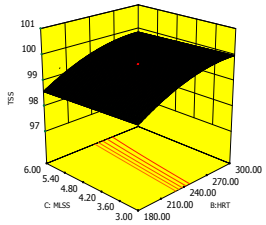

Fig. 5. 3-D plot from the model equation of MLSS and HRT effect on TSS removal.

The fouling rate under different specific *MLSS* concentrations in the feed wastewater is shown in Fig. 6. By comparing these findings with the results shown in Fig. 6, the great difference in the fluxes of wastewaters with *MLSS* concentration 3 and 4.5 g/L is obvious. It was observed that during experiments the flux for feed solution with *MLSS* concentration of 3 g/L becomes higher than that of 4 g/L. This fact suggests a higher tendency of suspended solids concentration to interact into membrane surface and also ability of air bubbling to enhanced the permeate flux. The flux values on submerged ultrafiltration for feed solution with increasing *MLSS* concentration become lower by 18 %. For both *MLSS* concentration, their foulings tend a quite different. Generally, the increase of membrane fouling with increasing *MLSS* concentration was found in many literatures by several reseachers, but some other studies have revealed no effect of *MLSS* concentration on fouling up to a threshold concentration [27].

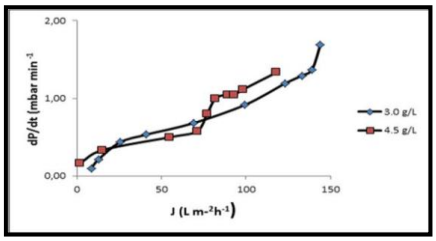

Fig. 6. The effects of different spesific of mixed liquor suspended solids concentration on permeate volume

3.2.2. Effect of aeration on membrane performance

The impact of aeration used in submerged membrane system was investigated, in which the continuous air bubble flow rate (ABFR) enhanced the membrane critical flux and thus minimized the fouling on the surface membrane. It is known that the membrane fouling can be considered from a critical flux point of view [28].

Fig. 6 shows the trend in *dP/dt* for various air bubbles flow rate. Significant variation is observed in terms of membrane permeability recovery, as expressed byn the recovery factor of *dP/dt*. The

results indicated that the use of air bubbles flow rate of 2.4 mL/min illustrated the increase of flux more than that of air bubbles flow rate of 1.2 and 3.0 mL/min. The degree supression of irreversible fouling was occured at air bubbles flow rate of 2.4 mL/min due to the achieved highest flux. Moreover, this would also mean that the aeration can be tuned according to the permeate flux to reduce the power consumption related to the air scouring.

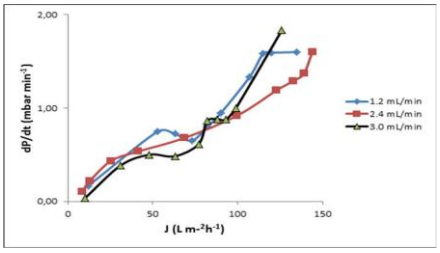

Fig. 6. The effects of different specific air bubble flow rates on permeate volume.

The results from RSM was showed in fig. 7 that the suspended solids removal increased with increasing ABFR from 1.20 ml/min to 2.40 ml/min, then decreased with further increasing of ABFR at maximum HRT of 300 min. TSS removal efficiency is obtained with the operating parameters as tabulated in Table 4. TSS removal efficiency is found to increase with an increase in ABFR from 1.2 ml/min to 2.1 ml/min and then decrease with further increased ABFR. It suggested this variable significantly affects the TSS removal.

However, further increase in ABFR resulted in a decrease in TSS removal. This is consistent with the conclusion made by Fu *et al.* (2007) [29]. Note that in Fig. 7, when the ABFR increased from 1.2 to 2.25 ml/min, TSS removal achieved the maximum value of thus the turbulent flow weakened the effect of concentration polarization in further increasing of ABFR. Although high ABFR could enhance the flux, forceful turbulent is not recommended in UF membrane process. An increase in the ABFR partly stimulated the fouling resistance, but there was a critical value beyond which the air bubbles flow rate increase had virtually no effect on the fouling resistance efficiency [30]. A higher shear rate due to extensive aeration can also have detrimental effects, as it increases the shear-induced diffusion and inertial lift forces for the large particles and causes small particle, which can induce severe pore blocking and irreversible gel formation to become the major foulants. Additionally, bubbles might be trapped in gas pockets between groups of fibers, minimizing effective membrane surface area. Ueda *et al.* (1997) observed a maximum aeration rate which a further increase has no effect on fouling supression beyond its critical value [31]. The turbulent flow may consume trans-membrane pressure of the system, causing weaker hydraulic and attachability factors which lead to the decline of the suspended solids removal.

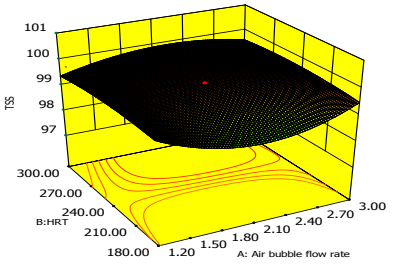

Fig. 7. 3-D plot from the model equation of effect the (ABFR) and hydraulic retention time (HRT).on TSS removal.

The removal of main parameters of permeate for refinery produced wastewater treatment has been calculated and listed in table 4. These results were achieved by using refinery produced wastewater with optimized process conditions of MLSS concentration of 3 g/L and ABFR of 2.4 ml/min.

Table 4: Optimum process conditions (factors) for maximum reponses with standard deviation (S.D.)

Parameters	Optimum value (S.D.)
ABFR, ml/min	2.4
HRT, min	276.93
MLSS, g/L	3.0
Flux, L/m^{3}h	148.82
TSS (%)	99.82

4. Conclusions

Submerged UF technique has been conducted to elucidate flux and fouling mechanism. PVDF UF membranes were fabricated via a dry-jet wet spinning method. Various concentrations of TiO_2 at constant value of $LiCl.H_2O$ were used as inorganic additives in the spinning dopes in order to improve the phase-inversion rate and provide porous asymmetric membranes with advanced structure for refinery produced wastewater treatment. Several characterizations and measurement techniques such as membrane structure, porosity, average pore size, and permeability were utilized to evaluate fine structural details of the membrane and membrane performance. Refinery wastewater filtration was conducted through in-house prepared PVDF hollow fiber UF membranes. FESEM and AFM images showed that MLSS concentration of 3.0 g/L and ABFR of 2.4 ml/min formed less fouling. Permeability test achieved significantly higher flux of 148.82 L/m^{3}h and removal of total suspended solids of 99.82% for refinery wastewater treatment.

References

[1] K.J. Howe, M.M. Clark, Fouling of microfiltration and ultrafiltration membranes by natural waters, Environ. Sci. Technol. 36 (16) (2002) 3571-3576.

[2] H. Huang, K. Schwab, J.G. Jacangelo, Pretreatment for low pressure membranes in water treatment: a review, Environ. Sci. Technol. 43 (9) (2009) 3011-3019.

[3] X.J. Huang, Z.K. Xu, L.S. Wang J.L. Wang, Surface modification of polyacrylonitrile-based membranes by chemical reactions to generate phospholipid moieties, Langmuir. 21(7) (2005) 2941-2947.

[4] T. Caroll, N.A. Booker, Axial features in the fouling of hollow-fibre membranes, J. Membr. Sci. 2000, 168 (1-2): 203-212.

[5] A.H. Nguyen, R.M. Narbaitz, T. Matsuura, Impacts of hydrophilic membrane additives on the ultrafiltration of river water, J. Environ.. Eng. ASCE. 133(5) (2007) 515-522.

[6] A. Bottino, G. Capanelli, S. Munari, A. Turturro, High performance ultrafiltration membranes cast from LiCl doped solution, Desalination. 1998, 68: 167-177.

[7] M. Khayet, T. Matsuura, Preparation and characterization of polyvinylidene fluoride membranes for membrane distillation, Ind. Eng.Chem. Res. 40 (2001) 5710-5718.

[8] A. Bottino, G. Capannelli, A. Comite, R. Mangano, Critical flux in submerged membrane bioreactors for municipal wastewater treatment, Desalination. 245 (2009) 748-753.

[9] B. Bienati, A. Bottino, G. Cappanelli, A. Comite, Characterization and performance of different types of hollow fibre membranes in a laboratory-scale MBR for the treatment of industrial wastewater, Desalination 231 (2008) 133-140.

[10] S. Chabot, C. Roy, G. Chowdhury, T. Matsuura, Development of poly(vinylidene fluoride) hollow fiber membranes for the treatment of water/organic vapor mixtures, J. Appl. Polym. Sci. 65 (1997) 1263-1270.

[11] X. Cao, J. Ma, X. Shi, Z. Ren, Effect of TiO_2 nanoparticle size on the performance of PVDF membrane, Appl. Surf. Sci. 253 (2006) 2003-2010.

[12] E. Yuliwati, A.F. Ismail, T. Matsuura, M.A. Kassim, M.S. Abdullah, Characterization of surface-modified porous PVDF hollow fibers for refinery wastewater treatment using microscopic observation, Desalination 283 (2011) 206-213.

[13] E. Yuliwati, A.F. Ismail, Effect of additives concentration on the surface properties and performance of PVDF ultrafiltration membranes for refinery wastewater treatment, Desalination 273 (2011) 226-234.

[14] Environmental Quality (Industrial Effluent) Regulation 2009, http://www.mkma.org/EnvironmentalRegulation2009.htm. , Retrieved on 25 May 2011.

[15] E. Yuliwati, A.F. Ismail, T. Matsuura, M.A. Kassim, M.S. Abdullah, Effect of modified PVDF hollow fiber submerged ultrafiltration membrane for refinery wastewater treatment. Desalination 283 (2011) 214-220.

[16] M. Khayet, C.Y. Feng, K.C. Khulbe, T. Matsuura, Preparation and characterization of polyvynilidene fluoride hollow fiber membranes for ultrafiltration, Polymer., 43 (2002) 1917-1935.

[17] Y.H. Zhao, Y.L. Qian, B.K. Zhu, Y.Y. Xu, Modification of porous poly(vinylidene fluoride) membrane using amphiphilic polymers with different structures in phase inversion process, J. Membr. Sci. 310(1-2) (2008) 567-576.

[18] B. van der Bruggen, C. Vandecasteele, T. van Gestel, W. Doyen, R. Leysen, A review of pressure-driven membrane processes in wastewater treatment and drinking water production, Environmental Progress. 22(1) (2003) 46-56.

[19] F. Wang, V.V. Barbara, Pore blocking mechanism during early stages of membrane fouling by colloids, J. Colloid Int. Sci. 328(2) (2008) 464-469.

[20] H. Yamamura, K. Kimura, T. Okajima, H. Tokumoto, Y. Watanabe, Affinity of functional groups for membrane surfaces: implications for physically irreversible fouling, Environmental and Science Technology 42(14) (2008) 5310-5315.A.W. Zularisam, A.F. Ismail, R. Salim, Behaviour of natural organic matter in membrane filtration for surface water treatment: a-review, Desalination 194 (2006) 211-231.

[21] S.S. Sablani, M.F.A. Goosen, R. Al-Belushi, M. Wilf, Concentration polarization in ultrafiltration and reverse osmosis: a critical review, Desalination 141 (2001) 269-289.

[22] S.J. Oh, N. Kim, Y. T. Lee, Preparation and characterization of PVDF/TiO_2 organic-inorganic composite membranes for fouling resistance improvement, J. Membr. Sci 345 (2011) 13-20.

[23] G.D. Profio, X. Ji, E. Curcio, E. Drioli, Submerged hollow fiber ultrafiltration as seawater pretreatment in the logic of integrated membrane desalination systems, Desalination 269 (2011) 128-135.

[24] K.C. Khulbe, C.Y. Feng, F. Hamad, T. Matsuura, M. Khayet, Structural and performance study of microporous polyetherimide hollow fiber membranes prepared at different air gap, J. Membr. Sci. 245 (2004) 191-198.

[25] R.H. Myers, D.C. Montgomery, Response Surface Methodology: Process and Product Optimization using Designed Experiments, 2nd ed., John Wiley & Sons, USA, 2002.

[26] Y. Mo, J. Chen, W. Xue, X. Huang, Chemical cleaning of nanofiltration membrane filtrating the effluent from a membrane bioreactor, Sep. Purif. Technol. 75 (2010) 407-414.

[27] R.J. Baker, A.G. Fane, C.J.D. Fell, B.H. Yoo, Factors affecting flux in crossflow filtration, Desalination 53 (1985) 81-93.

[28] D.P. Saroj, G. Guglielmi, D. Chiarani, G. Andreottola, Subcritical fouling behaviormodelling of membrane bioreactors for municipal wastewater treatment: The prediction of the time to reach critical operating condition, Desalination 231 (2008) 175-181.

[29] J. Fu, Y. Zhao, Q. Wu, Optimising photoelectrocatalytic oxidation of fulvic acid using response surface methodology, J. Hazard. Mat. 144 (2007) 499-505.

[30] P. Le-Clech, B. Jefferson, S.J. Judd, Impact of aeration, solid concentration and membrane characteristics on the hydraulic performance of a membrane bioreactor, J. Membr. Sci. 218 (2003) 117-129.

[31] T. Ueda, K. Hata, Treatment of domestic sewage from rural settlements by a membrane bioreactor, Water Sci. Technol. 34 (1996) 186-196.